Upregulation of eukaryotic translation initiation factor 3 subunit a promotes cell survival in ameloblastoma

Zhenjiang Ding, DDS, MS,[a,c] Jie Liu, PhD,[b] Junting Wang, MS,[c] Biying Huang, MS,[c] and Ming Zhong, DDS, PhD[c]

Objectives. This study aimed to detect the expression of eukaryotic translation initiation factor 3 subunit a (eIF3a) in ameloblastoma (AB) tissues compared with normal oral mucosa (NOM) tissues and investigate the roles of eIF3a in the immortalized ameloblastoma cell line (AM-1) cell proliferation and apoptosis.

Study Design. We performed immunohistochemistry to determine the expression of eIF3a in AB tissues (n = 83) and NOM tissues (n = 20). Real time−quantitative polymerase chain reaction and Western blot analyses were conducted with AB tissues (n = 30) and NOM tissues (n = 6). The correlation between eIF3a expression and the clinical/pathologic features of patients with AB is also presented. The functional role of eIF3a in AM-1 cells was assessed with lentiviral vector−mediated shRNA (small hairpin RNA).

Results. Our results indicated that eIF3a was significantly upregulated in AB. Additionally, eIF3a knockdown in AM-1 cells significantly inhibited cell proliferation and promoted apoptosis.

Conclusions. These data indicate that eIF3a facilitates the survival of AB cells and may serve as a promising therapeutic target in AB. (Oral Surg Oral Med Oral Pathol Oral Radiol 2019;128:146−153)

Ameloblastoma (AB) is a benign, osteolytic, slow-growing neoplasm that accounts for 9% to 11% of odontogenic tumors in humans.[1] Approximately 80% of ABs are found in the posterior mandible, and the remaining 20% originate from maxilla.[2,3] AB has no propensity toward age or gender, with a reported age range being 4 to 92 years and male-to-female occurrence ratio of 1.14:1.[4] AB is classified as ameloblastoma, unicystic ameloblastoma, and extraosseous/peripheral ameloblastoma according to the 4th edition of the *World Health Organization Classification of Head and Neck Tumors*.[5] Previously reported recurrence rates ranged from 8% to 38% for ameloblastoma,[6] 4% to 17% for unicystic ameloblastoma,[6] and 16% to 19% for extraosseous/peripheral ameloblastoma.[7] Many genes have been reported to exhibit dysregulated expression in AB, such as oncogenes (*c-Myc, FOS*, and *Ras*) and antioncogenes (*P53, APC*), which are associated with malignant tumors.[8]

In 1998, the immortalized ameloblastoma cell line (AM-1) was established by Harada et al., and this cell line maintained the epithelial cell morphology and expression of the cytokeratins K8, K14, K18, and K19, as well as Bcl-2 proteins.[9] In recent years, this cell line has been widely used in AB-related studies, allowing in vitro studies to investigate the pathogenesis of AB at a cellular level.

Abnormal regulation of gene expression may result in deregulated cell growth and tumorigenesis. Translation of messenger RNA (mRNA) is regulated by many eukaryotic translation initiation factors at the rate-limiting tumor initiation step.[10] Eukaryotic translation initiation factor 3 subunit a (eIF3a), as the largest subunit of the eIF3 complex, plays a key role in the establishment of ribosomes and the initiation of translation.[11] eIF3a has been implicated as a proto-oncogene and is related to cancer occurrence, metastasis, prognosis, and the therapeutic response.[12] eIF3a is overexpressed in carcinomas of the breast,[13] cervix,[14] lung,[15] stomach,[16] urinary bladder,[11] colon,[17] and pancreas.[18] Fibroblasts with ectopic expression of eIF3a acquire oncogenic properties, such as increased clonogenicity and attenuation of apoptosis.[19] Knocking down eIF3a in urinary[11] and pancreatic cancer cells[18] consistently impairs cell proliferation, colony formation, migration, and invasion. It is reported that eIF3a expression correlates with cell apoptosis of gastric cancer in humans.[16] Despite partial degradation, eIF3a plays a role in apoptotic cells by translocating to the cell surface and facilitating phagocytosis by macrophages.[20]

Statement of Clinical Relevance

Our study revealed that eukaryotic translation initiation factor 3 subunit a was markedly upregulated in ameloblastoma and that it can promote proliferation and inhibit apoptosis of ameloblastoma cells. Therefore, it could be a potential, novel target for treatment of ameloblastoma.

[a]Department of Pediatric Dentistry, School of Stomatology, China Medical University, Shenyang, Liaoning, China.
[b]Department of Central Laboratory, China Medical University, Shenyang, Liaoning, China.
[c]Department of Oral Histopathology, School of Stomatology, China Medical University, Shenyang, Liaoning, China.
Received for publication Oct 24, 2018; returned for revision Feb 1, 2019; accepted for publication Feb 13, 2019.

2212-4403/$-see front matter
https://doi.org/10.1016/j.oooo.2019.02.016

Because of the critical role of eIF3a in tumorigenesis and regulation, we designed the present study to investigate the roles of eIF3a in the proliferation and apoptosis of AM-1 cells. We also examined the correlation of eIF3a expression and its clinical/pathologic features in patients with AB with the aim of determining the possible mechanisms of eIF3a in tumorigenesis.

MATERIALS AND METHODS

Tissue samples

From 2015 to 2017, samples were obtained from 83 AB cases via surgical resection, and normal oral mucosa (NOM) tissues were collected from 20 patients undergoing mandibular third molar extraction from the Department of Oral and Maxillofacial Surgery, School of Stomatology, China Medical University. Thirty AB samples and 6 NOM samples were collected for real time−quantitative polymerase chain reaction (RT-qPCR) and Western blot analyses. All tissue samples were collected fresh from surgery, snap frozen in liquid nitrogen, and stored at −80°C. All experiments on human samples were approved by the Ethics Committee of the School of Stomatology, China Medical University, and informed consent was obtained from the donors.

Immunohistochemistry (IHC)

All AB and NOM tissues were fixed in 10% buffered formalin, embedded in paraffin, and cut into 4-μm-thick sections by using a standard sliding manual microtome. The sections were mounted onto glass slides and deparaffinized with xylene and rehydrated with a decreasing series of ethanol before antigen retrieval was performed by using a pressure cooker with citric acid buffer (pH 6.0). The endogenous peroxidase activity was inhibited by 3% hydrogen peroxide, and any cross-reaction with endogenous immunoglobulins was blocked with the use of 10% goat serum. The primary antibodies were rabbit anti-eIF3a (Abcam, Cambridge, MA) and rabbit immunoglobulin (IgG) (Vector, Burlingame, CA). The antibodies were applied separately and incubated overnight in a moist chamber at 4°C. The secondary antibody was goat anti-rabbit (Novus, Littleton, CO) and was added for 1 hour at room temperature. Then, the 3, 3'-diaminobenzidine substrate and hematoxylin were applied for staining. After dehydration, coverslips were fixed, and the slides were imaged. As a negative control, rabbit isotype IgG was applied as substitute for the primary antibody; for positive control, oral squamous cell carcinoma tissue was stained with the primary eIF3a antibody, which showed overexpression, as previously reported.[21]

Cytoplasmic and/or membrane staining intensities of parenchymal cells were evaluated under a light microscope (Olympus, Tokyo, Japan). The percentage of stained cells and the staining intensity were calculated in each sample by using IHC. The percentage of eIF3a−positive tumor cells was graded by using the following scale: 0 = negative (no positive staining); 1 = weak (1%−25% positive staining); 2 = moderate (26%−50% positive staining); 3 = strong (51%−75% positive staining); and 4 = high (76%−100% positive staining). The immunostaining intensity was rated as follows: 0 = none; 1 = weak; 2 = moderate; and 3 = intense. The final scores were calculated as the percentage rating multiplied by the intensity rating. In this scoring system, each component of the tumor was scored independently.

Real time−quantitative polymerase chain reaction

Total RNA from frozen tissues (AB and NOM) or AM-1 cells (lentiviral vector [LV] infected) was extracted separately by using the reagent Trizol (Invitrogen, Carlsbad, CA), according to the manufacturer's instructions. The purity and concentration of the extracted RNA were determined spectrophotometrically by measuring the ultraviolet absorbance at 260 and 280 nm. Complementary DNA was synthesized with an RT reagent kit (Takara, Dalian, China). A 20-μL master mixture of the RT reaction was incubated at 37°C for 15 minutes and at 85°C for 5 seconds, with 4 μL × 5 PrimeScript RT Master Mix and 1 μg total RNA and RNase-free water. Amplification was performed by using the SYBR Premix Ex Taq II kit (Takara, Dalian, China) with a qPCR system: 10 μL SYBR Premix Ex Taq II; 1 μL complementary DNA; 0.5 μL forward primer; 0.5 μL reverse primer; and 8 μL sterile purified water. The cycling conditions included a denaturation step at 95°C for 30 seconds, followed by 40 cycles of 95°C for 5 seconds and 60°C for 30 seconds. All steps were performed according to the Minimum Information for Publication of Quantitative Real-Time Polymerase Chain Reaction Experiments guidelines[22] and in triplicate. The following primer sequences were used for eIF3a and β-actin amplification:

- eIF3a Forward primer: 5′-ATAGTTGAAAAA-CAGCGTCG-3′
- Reverse primer: 5′-TAGAACCTTTGTGACTCGCT-3′
- β-actin Forward primer: 5′-CCATCGTCCACCG-CAAAT-3′
- Reverse primer: 5′-GCTGTCACCTTCACCGT TC-3′

The mRNA expression levels were determined by the cycle threshold normalized to β-actin expression by using the $2^{-\Delta\Delta Ct}$ formula.

Table I. The histopathologic types of ameloblastoma (AB) specimens (n = 83)

Types of AB	*n (%)*
AB	67 (80.72%)
Unicystic AB	8 (9.64%)
Extraosseous/peripheral AB	8 (9.64%)

Western blot

Total protein from frozen tissues (AB and NOM) or AM-1 cells (LV infected) was extracted separately by using the Total Protein Extraction Kit, according to the manufacturer's instruction (Wanleibio, Shenyang, China). AB specimens were sampled from the central area of the tumor.[23] Protein concentration was measured by using the bicinchoninic acid protein assay kit (Wanleibio, Shenyang, China). For each sample, 80 μg of protein in 20 μL solution was separated on an 8% sodium dodecyl sulfate-polyacrylamide gel electrophoresis gel. Protein was then transferred to a polyvinylidene fluoride or polyvinylidene difluoride membrane (Sigma, Shanghai, China). The membranes were blocked with 5% nonfat dry milk and 0.1% Tween-20 for 1 hour. The membranes were then incubated overnight with primary antibodies at 4°C. Anti-eIF3a (Abcam, Cambridge, MA) was used as the primary antibody. Anti-β-actin antibody (Sigma-Aldrich, St. Louis, MO) or anti-glyceraldehyde 3-phosphate dehydrogenase antibody (Abcam, Cambridge, MA) was used as the internal control. A goat antirabbit antibody (Novus Bio, Littleton, CO) was used as the secondary antibody. Immunoreactive proteins were detected with Pierce enhanced chemiluminescence Western Blotting Substrate (Pierce, Rockford, IL). Image-Pro Plus software was used for quantitative analysis.

Cell culture

The human ameloblastoma cell line AM-1 was obtained from Dr. Hidemitsu Harada (School of Dentistry, Iwate Medical University, Japan). The cells between passages 15 and 25 were seeded in plates or flasks in keratinocyte serum-free medium (Gibco-Invitrogen, Carlsbad, CA) at a density of 10^5 cells/cm^2, and the adhering cells were cultured and maintained at 37°C in a humidified atmosphere containing 5% carbon dioxide. The growth and morphology of cultured cells were observed under an inverted microscope.

Generation of LVs expressing eIF3a, shRNA, and AM-1 infection

eIF3a shRNA and negative control shRNA were designed, synthesized, and ligated into the GV115-EGFP vector before packaging in 293 T cells (Genechem, Shanghai, China). AM-1 cells were infected with lentivirus, according to the manufacturer's protocol (Genechem, Shanghai, China). The infection efficiency was evaluated by green fluorescent protein expression 3 days after LV infection.

The negative control sequence has previously been used in a number of studies and has no significant homology to any human gene sequences.[24,25] The following primer target sequences were designed:

- sheIF3a target sequence: 5′-GGCAGAAGAA-CAAATGCTA-3′
- shCtrl target sequence: 5′-TTCTCCGAACGTGT-CACGT-3′

Colony formation assay

AM-1 cells were seeded in 6-well plates (1000 cells/well) 3 days after LV infection. After 14 days of incubation, 4% paraformaldehyde was added for fixation,

Table II. The relevance between eIF3a expression and clinical/pathologic features of AB patients (n = 83)

Features	*n (%)*	*eIF3a expression (IHC scores)*	*P values*
Gender			0.0492*
Male	52 (62.65%)	8.25 ± 3.86	
Female	31 (37.35%)	9.90 ± 3.25	
Age			0.7989
≤50 years	62 (74.70%)	8.81 ± 3.85	
>50 years	21 (25.30%)	9.05 ± 3.35	
Location			0.4541
Maxilla	13 (15.66%)	8.15 ± 3.72	
Mandible	70 (84.34%)	9.00 ± 3.73	
Status			0.5463
Primary	67 (80.72%)	8.75 ± 3.87	
Recurrent	16 (19.28%)	9.38 ± 3.05	

*$P < .05$; *AB,* ameloblastoma; *eIF3a,* eukaryotic translation initiation factor 3, subunit a; *IHC,* immunohistochemistry.

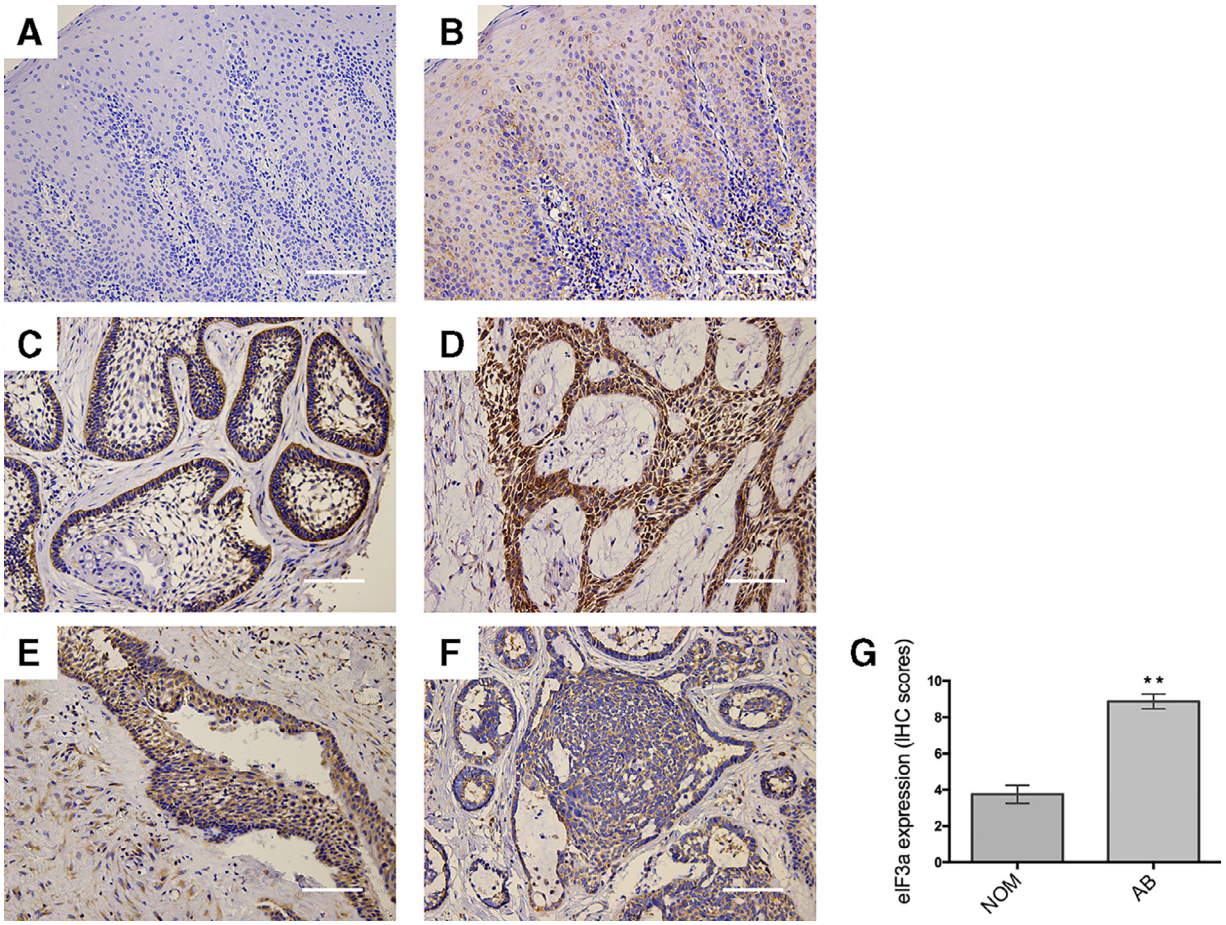

Fig. 1. Representative images of immunohistochemistry (IHC) staining and the analysis of eukaryotic translation initiation factor 3, subunit a (eIF3a) expression in normal oral mucosa (NOM) and ameloblastoma (AB) tissues. NOM tissue (negative control) **(A)**, NOM tissue **(B)**, AB tissue (follicular pattern) **(C)**, AB tissue (plexiform pattern) **(D)**, AB tissue (unicystic type) **(E)**, and AB tissue (extraosseous/peripheral type) **(F)**. (magnification × 200; scale bar = 100 μm). eIF3a was expressed in the cytoplasm and membranes and showed weak to moderate expression in NOM tissues but high expression in AB tissues. The IHC scores of eIF3a expression in NOM and AB are shown as histograms **(G)**. The expression of eIF3a was significantly increased in AB tissues compared with NOM tissues. (**$P < .01$; Error bars indicate the standard error of the IHC scores based on 20 NOM and 83 AB tissues). *A high-resolution version of the image A, B, C, D, E, and F for use with the Virtual Microscope is available as eSlide: VM05593, VM05594, VM05595, VM05597, VM05598, and VM05599.*

and Giemsa was added for staining. Colonies containing greater than 50 individual cells were counted, and all experiments were conducted in triplicate. The colonies were counted under a microscope (Olympus, Tokyo, Japan) and captured.

3-(4,5-dimethythiazol-. 2-yl)-2,5-diphenyl tetrazolium bromide (MTT) assay

MTT assay is a quantitative and sensitive detection method for cell proliferation by measuring the metabolic activity and growth rate of the cells. To detect the effect of eIF3a on AM-1 cell proliferation and viability, thiazolyl blue (MTT) (Genview, Beijing, China) was used, according to the manufacturer's protocols. AM-1 cells were seeded in 96-well plates (1500 cells/well) 3 days after LV infection. The MTT assay was conducted according to the manufacturer's protocols (Genview, Beijing, China). The optical density 490 values were measured at days 1, 2, 3, 4, and 5.

Flow cytometry analysis of cell apoptosis

Cell apoptosis was evaluated with the Annexin V-APC kit (eBioscience, San Diego, CA) according to the manufacturer's instructions. After 5 days of LV infection with sheIF3a or shCtrl, infected cells were trypsinized, washed with D-Hanks buffer and × 1 binding buffer. Next, they were stained in 200 μL cell suspension buffer with 10 μL annexin V-APC for 10 to 15 minutes at room temperature in the dark. The percentage of apoptotic cells was analyzed by flow cytometry in triplicate. The overall apoptotic rate was equal to the sum of the late apoptotic percentage (UR: upper right

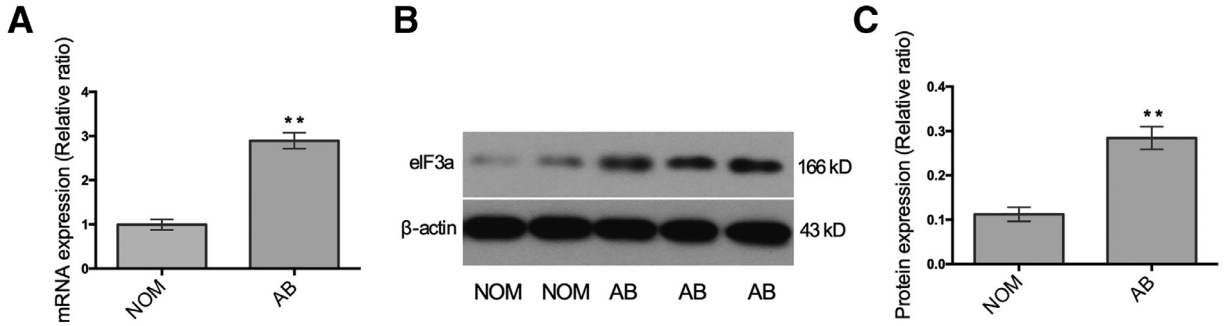

Fig. 2. Expression of eukaryotic translation initiation factor 3, subunit a (eIF3a) in ameloblastoma (AB) and normal oral mucosa (NOM) tissues. Real time−quantitative polymerase chain reaction (RT-qPCR) showed that the messenger RNA (mRNA) level of eIF3a was significantly higher in AB tissues than that in NOM tissues **(A)**. Western blot analysis showed that the expression of eIF3a was also significantly higher in AB tissues compared with that in NOM tissues at the protein level **(B, C)**. (**$P < .01$; Error bars indicate the standard error).

quadrant) and the early apoptotic percentage (LR: lower right quadrant).

Statistical analysis

The software SPSS version 17.0 (SPSS Inc., Chicago, IL) was used to perform statistical analyses. Comparisons between 2 groups were performed with independent 2-tailed Student *t* tests, and comparisons among >2 groups were performed with 1-way analysis of variance. All *P* values < .05 were considered statistically significant.

RESULTS

Association between eIF3a expression and the clinical/pathologic features of AB

The histopathologic subtypes of AB specimens used in our study are presented in Table I. The data indicate that approximately 80% of the specimens were AB, nearly 10% of the samples were unicystic, and 10% were extraosseous/peripheral.

The association between eIF3a expression and the clinical/pathologic features of patients with AB is shown in Table II. The level of eIF3a expression was significantly greater in females than in males ($P = .0492$). The differences between the other parameters were not statistically significant. The ages of patients with AB ranged from 6 and 88 years, and the average age at the time of diagnosis was 38.2 years.

eIF3a is upregulated in AB tissues

In our study, staining of the subcellular localizations showed that the majority of eIF3a was located in the cytoplasm, and the remainder of eIF3a was membrane bound. NOM tissues expressed weak to moderate immunoreactivity to eIF3a compared with no signal in the isotype IgG-negative control group. In contrast, AB tissues expressed strong immunoreactivity to eIF3a antibody. Representative image of IHC staining of IgG expression in NOM tissue is shown in Figure 1A, and the eIF3a expression in NOM and AB tissues are shown in Figures 1B through 1F. The IHC scores of eIF3a expression in NOM and AB tissues are shown as histograms (Figure 1G). Statistical analysis showed that eIF3a expression in AB tissues was significantly higher than in NOM tissues at the protein level. ($P < .01$).

The mRNA level of eIF3a was significantly increased in AB compared with NOM tissues ($P < .01$) (Figure 2A). Furthermore, the results of the Western blot analysis were consistent with the results of the RT-qPCR analysis ($P < .01$) (Figures 2B and 2C).

Knockdown of eIF3a suppresses proliferation and induces apoptosis of AM-1 cells

LV-mediated knockdown was conducted to inhibit eIF3a expression in AM-1 cells. The infection efficiency and cell morphology were observed 3 days after LV infection (Figure 3A). The results of a RT-qPCR analysis demonstrated that the mRNA expression of eIF3a was significantly decreased in AM-1 cells in the sheIF3a group (Figure 3B). Moreover, representative images clearly show a reduction of eIF3a protein expression after sheIF3a transfection in AM-1 cells (Figure 3C).

A colony formation assay was conducted to assess cell clonogenicity (Figure 3D). The sheIF3a group had a statistically significant decrease in the number of colony formation compared with the control group ($P < .01$) (Figure 3E). Additionally, the MTT assay demonstrated that after silencing eIF3a expression, AM-1 cells exhibited decreased cellular metabolic activity (Figure 3F). Thus, eIF3a knockdown suppresses the proliferation and cellular metabolic activity of AM-1 cells.

A flow cytometric analysis was conducted to further investigate the role of eIF3a on apoptosis regulation. The average rate of apoptosis was 3.68% (UR: 3.14%; LR: 0.54%) in the shCtrl group, and 7.89% (UR: 5.64%; LR: 2.25%) in the sheIF3a group (Figure 3G). As shown in Figure 3H, apoptosis was significantly

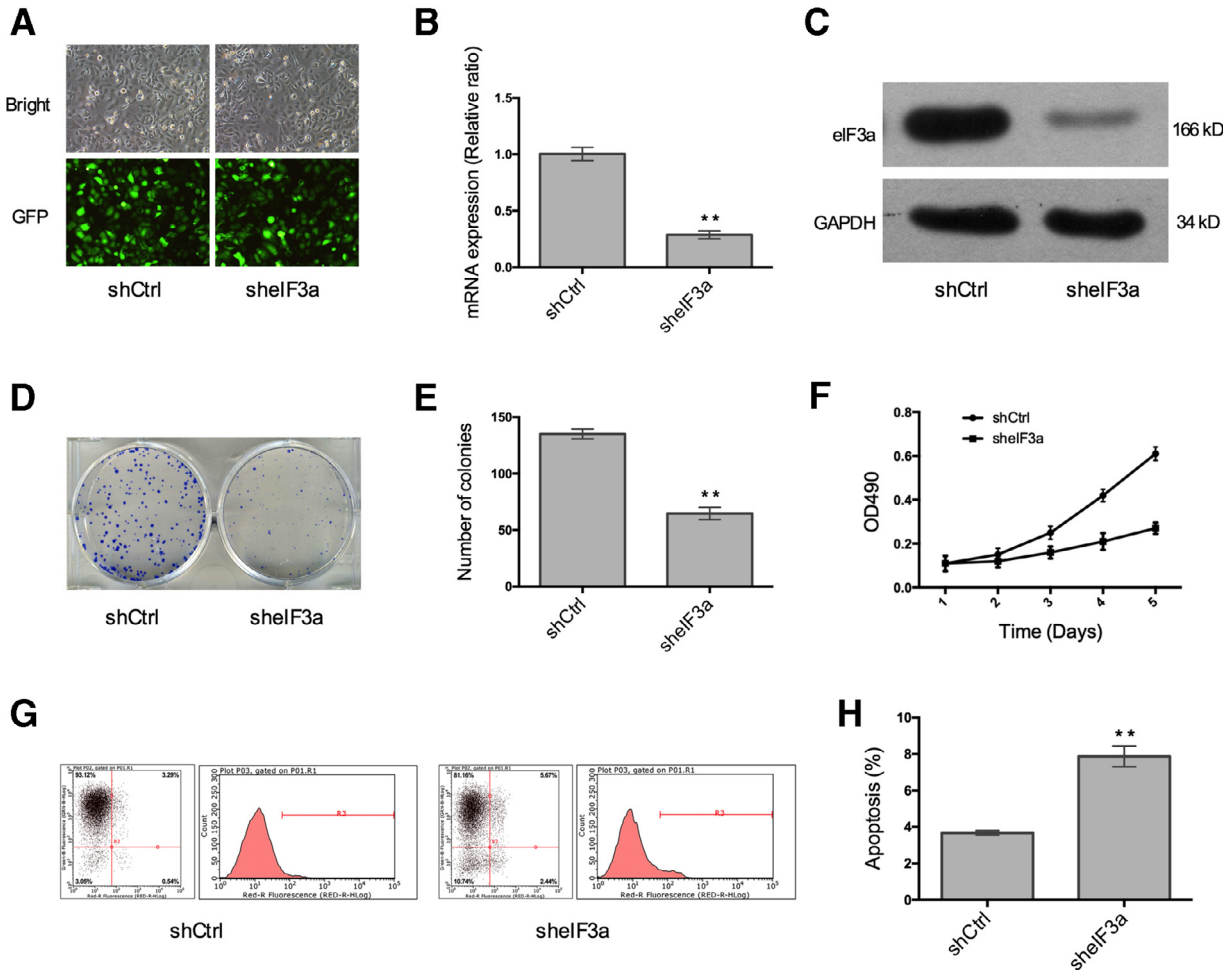

Fig. 3. Eukaryotic translation initiation factor 3, subunit a (eIF3a) knockdown and the effects of cell proliferation and apoptosis by small hairpin eukaryotic translation initiation factor 3, subunit a (sheIF3a). Representative images of eIF3a knockdown in immortalized ameloblastoma cell line (AM-1) cells (magnification × 100) **(A)**. Analysis of eIF3a after the knockdown in AM-1 cells at the messenger RNA (mRNA) level, as assessed by real time−quantitative polymerase chain reaction (RT-qPCR) analysis **(B)**. Western blot of eIF3a knockdown in AM-1 cells at the protein level **(C)**. Representative images of colony formation **(D)** and histograms indicate the average cell count values in AM-1 cells infected with small hairpin control (shCtrl) and sheIF3a **(E)**. The cumulative data of cellular metabolic activity with infected AM-1 cells were analyzed by using the 3-(4,5-dimethythiazol-. 2-yl)-2,5-diphenyl tetrazolium bromide (MTT) assay, data represent the mean optical density (OD) 490 values and standard error of three independent experiments **(F)**. Flow cytometry was used to analyze apoptosis in AM-1 cells after infection; the average rate of apoptosis was equal to the sum of the late apoptotic percentage (upper right quadrant [UR]) and the early apoptotic percentage (lower right quadrant [LR]) **(G)**, and representative histograms of the results are shown **(H)**. (**$P < .01$; Error bars indicate the standard error).

accelerated in AM-1 cells in the sheIF3a group compared with the shCtrl group ($P < .01$), suggesting the antiapoptotic role of eIF3a in AM-1 cells.

DISCUSSION

The most prevalent odontogenic tumor in developing countries is AB, which constitutes 14% of all tumors and cysts in the maxilla and the mandible.[26,27] The age range of patients with AB is 0 to 98 years, and the average age is estimated to be 42.3 years in Europe and 30.4 in Africa.[28,29] In addition, Reichart et al. reported that the median age was 35 years (range 4−92 years), and the male-to-female incidence ratio was 1.14:1.[4] Consistent with the results of Reichart et al., the average age in our study was 38.2 years and the age range was 6 to 88 years. The male to female incidence ratio in our study was 1.68:1, which is higher than the previously reported ratios. Moreover, the incidence of AB in the pediatric population, according to our data, was 8.4%, which is much lower than the 15.2% reported by Bansal et al.[30] Other findings, including lesion location and status, were consistent with those of previous studies.

In this study, we found that eIF3a expression was significantly elevated in AB tissues compared with NOM tissues in humans at the protein and mRNA levels. Increased eIF3a expression at the protein and mRNA levels has been demonstrated in malignant tumors. This study, to our knowledge, is the first to report increased eIF3a expression in human AB lesions. However, we did not observe a statistically significant difference in eIF3a expression levels between primary and recurrent AB lesions (see Table I). Although this does not rule out a potential role of eIF3a in AB recurrence, it does demonstrate that primary and recurrent AB lesions have similarly aberrant eIF3a activity. In addition, studies have shown that overexpression of eIF3a is sufficient to induce malignant transformation of fibroblasts in vitro.[19] Further studies may demonstrate a link between consistently elevated eIF3a expression and malignant transformation of AB.

Lee et al. demonstrated that binding of eIF3a to specific cell-proliferation mRNA via the mRNA 5' untranslated region could be targeted to control carcinogenesis.[31] eIF3 is the largest complex factor of all eIFs and contains 13 subunits, consisting of 1 octamer core (a, c, e, f, h, l, k, and m) and 5 peripheral (b, d, g, i, and j) subunits.[12] Among them, eIF3a is the largest subunit and has been widely and extensively investigated. eIF3a has been reported to be a proto-oncogene correlated with tumor occurrence and metastasis that is driven by uncontrolled proliferation.[12] Recent studies have demonstrated that pathogenesis of AB involves multiple genes involved in proliferation, such as *Periostin, WNT1, MCM3, c-Myc*, and *Survivin*.[32-36] However, the functional contribution of eIF3a in AB cell proliferation and apoptosis has not been elucidated. Therefore, we examined the impact of eIF3a knockdown in AM-1 cell proliferation and apoptosis. We demonstrated that eIF3a knockdown reduced the proliferative capacity of AM-1 cells and promoted apoptosis (see Figure 3). Inhibition of uncontrolled proliferation and induction of apoptosis are critical components of tumor treatment and regression.[37] Our results suggest that eIF3a pathologically promotes proliferation and prevents apoptosis of AB cells, which is consistent with the locally invasive, although benign, nature of AB in vivo. Similar to our findings, eIF3a knockdown has been shown to inhibit proliferation and clonogenic potential of urinary bladder cancer cell lines.[11]

Studies have demonstrated a number of specific gene mutations found in AB. *B-RAF*^{V600E} mutation was the most common mutation identified in AB[38] and in the AM-1 cell line.[39] Under normal conditions, eIF3a interacts with Raf-1 and appears to interfere with its function,[40] but it is unknown how eIF3a may interact with mutated B-RAF or how its overexpression in a tumor environment may alter physiologic extracellular signal-related kinase pathways. Two other mutations in *RAS* and *FGFR2* in mitogen-activated protein kinase signaling were also identified, which suggested that the activation of the mitogen-activated protein kinase pathway likely represented a critical event and occurred early in the pathogenesis of AB.[41] However, the relationship between eIF3a and these mutations is unclear and needs further investigation.

CONCLUSIONS

Our data revealed that eIF3a was considerably upregulated in AB, and further analysis indicated that eIF3a played an important role in the survival of AB cells. These findings suggest that targeting eIF3a may be a promising strategy in the treatment of AB.

DISCLOSURE

This work was supported by grants from the National Natural Science Foundation of China (81072197 and 81470758), Science and Technology Research Project of Liaoning Provincial Education Department (LK201626), and Youth Science and Technology Innovation Talent Support Project of Shenyang (RC170078).

REFERENCES

1. Masthan KM, Anitha N, Krupaa J, Manikkam S. Ameloblastoma. *J Pharm Bioallied Sci*. 2015;7:S167-S170.
2. Becelli R, Carboni A, Cerulli G, Perugini M, Iannetti G. Mandibular ameloblastoma: analysis of surgical treatment carried out in 60 patients between 1977 and 1998. *J Craniofac Surg*. 2002;13:395-400.
3. Kostic A, Jurisic A. X-ray diagnosis of ameloblastoma. *Dentomaxillofac Radiol*. 1972;1:47-50.
4. Reichart PA, Philipsen HP, Sonner S. Ameloblastoma: biological profile of 3677 cases. *Eur J Cancer B Oral Oncol*. 1995;31:86-99.
5. El-Naggar A, Chan J, Grandis J, Takata T, Slootweg P. WHO *Classification of Head and Neck Tumours*. ed. 4 Lyon, France: IARC; 2017.
6. Antonoglou GN, Sandor GK. Recurrence rates of intraosseous ameloblastomas of the jaws: a systematic review of conservative versus aggressive treatment approaches and meta-analysis of non-randomized studies. *J Craniomaxillofac Surg*. 2015;43:149-157.
7. Philipsen HP, Reichart PA, Nikai H, Takata T, Kudo Y. Peripheral ameloblastoma: biological profile based on 160 cases from the literature. *Oral Oncol*. 2001;37:17-27.
8. Kumamoto H. Molecular pathology of odontogenic tumors. *J Oral Pathol Med*. 2006;35:65-74.
9. Harada H, Mitsuyasu T, Nakamura N, et al. Establishment of ameloblastoma cell line, AM-1. *J Oral Pathol Med*. 1998;27:207-212.
10. Saletta F, Suryo Rahmanto Y, Richardson DR. The translational regulator eIF3a: the tricky eIF3 subunit! *Biochim Biophys Acta*. 2010;1806:275-286.
11. Spilka R, Ernst C, Bergler H, et al. eIF3a is over-expressed in urinary bladder cancer and influences its phenotype independent of translation initiation. *Cell Oncol*. 2014;37:253-267.

12. Yin JY, Zhang JT, Zhang W, Zhou HH, Liu ZQ. eIF3a: a new anticancer drug target in the eIF family. *Cancer Lett*. 2018;412:81-87.
13. Bachmann F, Banziger R, Burger MM. Cloning of a novel protein overexpressed in human mammary carcinoma. *Cancer Res*. 1997;57:988-994.
14. Dellas A, Torhorst J, Bachmann F, Banziger R, Schultheiss E, Burger MM. Expression of p150 in cervical neoplasia and its potential value in predicting survival. *Cancer*. 1998;83:1376-1383.
15. Pincheira R, Chen Q, Zhang JT. Identification of a 170-kDa protein over-expressed in lung cancers. *Br J Cancer*. 2001;84:1520-1527.
16. Chen G, Burger MM. p150 overexpression in gastric carcinoma: the association with p53, apoptosis and cell proliferation. *Int J Cancer*. 2004;112:393-398.
17. Haybaeck J, O'Connor T, Spilka R, et al. Overexpression of p150, a part of the large subunit of the eukaryotic translation initiation factor 3, in colon cancer. *Anticancer Res*. 2010;30:1047-1055.
18. Wang SQ, Liu Y, Yao MY, Jin J. Eukaryotic translation initiation factor 3a (eIF3a) promotes cell proliferation and motility in pancreatic cancer. *J Korean Med Sci*. 2016;31:1586-1594.
19. Zhang L, Pan X, Hershey JW. Individual overexpression of five subunits of human translation initiation factor eIF3 promotes malignant transformation of immortal fibroblast cells. *J Biol Chem*. 2007;282:5790-5800.
20. Nakai Y, Shiratsuchi A, Manaka J, et al. Externalization and recognition by macrophages of large subunit of eukaryotic translation initiation factor 3 in apoptotic cells. *Exp Cell Res*. 2005;309:137-148.
21. Spilka R, Laimer K, Bachmann F, et al. Overexpression of eIF3a in squamous cell carcinoma of the oral cavity and its putative relation to chemotherapy response. *J Oncol*. 2012;2012:901956.
22. Bustin SA, Benes V, Garson JA, et al. The MIQE guidelines: minimum information for publication of quantitative real-time PCR experiments. *Clin Chem*. 2009;55:611-622.
23. Garcia-Munoz A, Rodriguez MA, Liceaga-Escalera C, et al. Expression of the transcription factor PITX2 in ameloblastic carcinoma. *Arch Oral Biol*. 2015;60:799-803.
24. Ke Y, Bao T, Zhou Q, et al. Discs large homolog 5 decreases formation and function of invadopodia in human hepatocellular carcinoma *via* Girdin and Tks5. *Int J Cancer*. 2017;141:364-376.
25. Xie H, Huang S, Li W, Zhao H, Zhang T, Zhang D. Upregulation of Src homology phosphotyrosyl phosphatase 2 (Shp2) expression in oral cancer and knockdown of Shp2 expression inhibit tumor cell viability and invasion in vitro. *Oral Surg Oral Med Oral Pathol Oral Radiol*. 2014;117:234-242.
26. Lasisi TJ, Adisa AO, Olusanya AA. Appraisal of jaw swellings in a Nigerian tertiary healthcare facility. *J Clin Exp Dent*. 2013;5:e42-e47.
27. Oginni FO, Stoelinga PJ, Ajike SA, et al. A prospective epidemiological study on odontogenic tumours in a black African population, with emphasis on the relative frequency of ameloblastoma. *Int J Oral Maxillofac Surg*. 2015;44:1099-1105.
28. Oomens MA, van der Waal I. Epidemiology of ameloblastomas of the jaws: a report from The Netherlands. *Med Oral Patol Oral Cir Bucal*. 2014;19:e581-e583.
29. Olusanya AA, Adisa AO, Lawal AO, Arotiba JT. Gross surgical features and treatment outcome of ameloblastoma at a Nigerian tertiary hospital. *Afr J Med Med Sci*. 2013;42:59-64.
30. Bansal S, Desai RS, Shirsat P, Prasad P, Karjodkar F, Andrade N. The occurrence and pattern of ameloblastoma in children and adolescents: an Indian institutional study of 41 years and review of the literature. *Int J Oral Maxillofac Surg*. 2015;44:725-731.
31. Lee AS, Kranzusch PJ, Cate JH. eIF3 targets cell-proliferation messenger RNAs for translational activation or repression. *Nature*. 2015;522:111-114.
32. Kang Y, Liu J, Zhang Y, et al. Upregulation of Periostin expression in the pathogenesis of ameloblastoma. *Pathol Res Pract*. 2018;214:1959-1965.
33. Wang GN, Zhong M, Chen Y, Ji J, Gao XQ, Wang TF. Expression of WNT1 in ameloblastoma and its significance. *Oncol Lett*. 2018;16:1507-1512.
34. Jaafari-Ashkavandi Z, Mehranmehr F, Roosta E. MCM3 and Ki67 proliferation markers in odontogenic cysts and ameloblastoma. *J Oral Biol Craniofac Res*. 2019;9:47-50.
35. Duan L, Wu Y, Liang Y, Wan D, Zhang D, Zhang B. MiRNA-516 b inhibits ameloblastoma cell proliferation and invasion by regulating MYCBP/c-myc/RECK/MMP pathway. *Translational Cancer Research*. 2017;6:667-678.
36. González-González R, Molina-Frechero N, Damian-Matsumura P, Salazar-Rodriguez S, Bologna-Molina R. Immunohistochemical expression of Survivin and its relationship with cell apoptosis and proliferation in ameloblastomas. *Disease markers*. 2015;2015:301781.
37. Pratheeshkumar P, Raphael TJ, Kuttan G. Nomilin inhibits metastasis via induction of apoptosis and regulates the activation of transcription factors and the cytokine profile in B16 F-10 cells. *Integr Cancer Ther*. 2012;11:48-60.
38. Kurppa KJ, Caton J, Morgan PR, et al. High frequency of *BRAF V600 E* mutations in ameloblastoma. *J Pathol*. 2014;232:492-498.
39. Sweeney RT, McClary AC, Myers BR, et al. Identification of recurrent *SMO* and *BRAF* mutations in ameloblastomas. *Nat Genet*. 2014;46:722-725.
40. Xu TR, Lu RF, Romano D, et al. Eukaryotic translation initiation factor 3, subunit a, regulates the extracellular signal-regulated kinase pathway. *Mol Cell Biol*. 2012;32:88-95.
41. Brown NA, Rolland D, McHugh JB, et al. Activating *FGFR2-RAS-BRAF* mutations in ameloblastoma. *Clin Cancer Res*. 2014;20:5517-5526.

Reprint requests:

Ming Zhong
Department of Oral Histopathology
School of Stomatology
China Medical University
117 North Nanjing Street
Shenyang, Liaoning 110002
China.
Mzhong@cmu.edu.cn